GEOPHYSICAL RESEARCH LETTERS, VOL. 40, 290–294, doi:10.1002/grl.50131, 2013

Thermal elasticity of $(Fe_x,Mg_{1-x})_2SiO_4$ olivine and wadsleyite

M. Núñez-Valdez,[1] Z. Wu,[2] Y. G. Yu,[3] and R. M. Wentzcovitch[4]

Received 3 July 2012; revised 28 December 2012; accepted 2 January 2013; published 31 January 2013.

[1] We present first-principles results for elastic moduli (bulk, K, and shear, G) and acoustic velocities (compressional, V_P, shear, V_S, and bulk V_Φ) of olivine (α) and wadsleyite (β) $(Fe_x,Mg_{1-x})_2SiO_4$, at high pressure (P) and temperature (T) with varying iron content ($0 \le x \le 0.125$). Pressure and temperature derivatives of these properties are analyzed. We show that adding 12.5% of Fe in forsterite softens V_P and V_S by ~3–6%, the same effect as raising temperature by ~1000 K in dry olivine at 13.5 GPa—the same is true in wadsleyite. This study suggests that Fe is effective in producing seismic velocity heterogeneity at upper mantle and transition zone conditions and should be another key ingredient, in addition to temperature and water content variations, in interpreting seismic heterogeneities in the transition zone. The effect of Fe on density, elastic, and velocity contrasts across the $\alpha \rightarrow \beta$ transition is also addressed at relevant conditions. We show that simultaneous changes of composition, temperature, and pressure do not affect significantly the relative density contrasts. We also find that compressional and shear impedance contrasts result primarily from velocity discontinuities rather than density discontinuity. **Citation:** Núñez-Valdez, M., Z. Wu, Y. G. Yu, and R. M. Wentzcovitch (2013), Thermal elasticity of $(Fe_x,Mg_{1-x})_2SiO_4$ olivine and wadsleyite, *Geophys. Res. Lett.*, *40*, 290–294, doi:10.1002/grl.50131.

1. Introduction

[2] Wadsleyite (β-phase) is a high-pressure polymorph of olivine (α-phase), $(Mg_{1-x},Fe_x)_2SiO_4$. These minerals are the main constituents of the Earth's upper mantle (UM) and upper transition zone (TZ) in pyrolitic lithologies [*Ringwood*, 1975; *Irifune and Ringwood*, 1987; *Putnis*, 1992]. At ~13.5 GPa, the $\alpha \rightarrow \beta$ transformation takes place near 1700 K [*Akaogi et al*., 1989; *Katsura and Ito*, 1989; *Brown and Shankland*, 1981]. This transformation is associated with the 410 km seismic discontinuity in the Earth. Interpretation of seismic data of this region in terms of mineralogy and chemical composition requires detailed knowledge of bulk (K) and shear (G) moduli as a function of pressure (P) and temperature (T) of constituent minerals [*Li and Liebermann*, 2007]. The dependence of seismic velocities on T and chemical composition at mantle conditions is of particular interest to interpret, for example, lateral shear-wave velocity (V_S) variations in the TZ region [see e.g., *Meier et al*., 2009]. So far, the elasticity database for minerals in the TZ is still incomplete, especially for those containing Fe, Al, and Ca. In the past two decades, much experimental effort has been devoted to understanding the effect of adding iron on elasticity of minerals, and quite a few techniques have been used to measure elasticity of olivine and wadsleyite, including Brillouin spectroscopy [*Zha et al*., 1998], ultrasonic interferometry [*Li and Liebermann*, 2000; *Liu et al*., 2005, 2009], resonant ultrasound spectroscopy and resonant sphere techniques [*Isaak*, 1992; *Mayama et al*., 2004; *Isaak et al*., 2010], impulsively stimulated laser scattering [*Abramson et al*., 1997], etc. However, different experimental conditions and the lack of a unified uncertainty scale on available experimental data disallow an accurate extraction of the effect of iron on elasticity at conditions of the 410 km seismic discontinuity. Previous computations on elasticity of α- and β-$(Mg_{1-x},Fe_x)_2SiO_4$ were limited to static calculations (0 K) [*Núñez Valdez et al*., 2010, 2011; *Stackhouse et al*., 2010], and simple extrapolations to high T do not work well because T-derivatives of K and G usually decrease in magnitude with increasing P (see section 3.1). In the past, thermal elastic properties of MgO and $MgSiO_3$-perovskite have been calculated by first principles using the quasi-harmonic approximation (QHA), valid up to ~2/3 of the melting temperature [e.g., *Karki et al*., 1999; *Wentzcovitch et al*., 2004], or using molecular dynamics [e.g., *Oganov et al*., 2001; *Li et al*., 2006]. Both methods demand enormous computational efforts. For example, QHA calculations have required vibrational density of states (VDoS) for strained atomic configurations at several P's, usually summing to about 1000 parallel jobs [*Da Silva et al*., 2007; *Da Silveira et al*., 2008]. As such, reports on high P-T thermal elasticity calculations of mantle minerals have been scanty. Here we use a new semi-analytical method [*Wu and Wentzcovitch*, 2008, 2011] to calculate K, G and compressional (V_P), shear (V_S), and bulk (V_Φ) velocities of α-β-$(Mg_{1-x},Fe_x)_2SiO_4$. This approach uses only static elastic constants and phonon density of states for unstrained configurations, therefore reducing computational time, resources, and especially manpower, by 1 to 2 orders of magnitude. We distinguish the effect of Fe from that of T on elasticity and acoustic velocities, and the two effects are compared. We then address the contrasts' behavior across the $\alpha \rightarrow \beta$ $(Fe_x,Mg_{1-x})_2SiO_4$ transition near conditions of the 410 km seismic discontinuity.

2. Theory

[3] Adiabatic elastic constants were obtained using the relation $C^S_{ijkl} = C^T_{ijkl} + \frac{T}{VC_V}\frac{\partial S}{\partial e_{ij}}\frac{\partial S}{\partial e_{kl}}\delta_{ij}\delta_{kl}$, where C_V is heat

[1]School of Physics and Astronomy, University of Minnesota, Minneapolis, Minnesota, USA.
[2]School of Earth and Space Sciences, University of Science and Technology of China, Hefei, Anhui, China.
[3]Department of Chemical Engineering and Materials Science, University of Minnesota, Minneapolis, Minnesota, USA.
[4]Department of Chemical Engineering and Materials Science, Minnesota Supercomputing Institute (MSI), University of Minnesota, Minneapolis, Minnesota, USA.

Corresponding author: M. Núñez-Valdez, School of Physics and Astronomy, University of Minnesota, Minneapolis, MN, USA. (valdez@physics.umn.edu)

©2013. American Geophysical Union. All Rights Reserved.
0094-8276/13/10.1002/grl.50131

capacity and V, S, and e are volume, entropy, and strain, respectively. C^T_{ijkl} are isothermal elastic constants calculated as strain derivatives of the Gibbs free energy, $C^T_{ijkl} = \left[\frac{\partial^2 G(P,T)}{\partial e_{ij}\partial e_{kl}}\right]_{P,T}$ [*Wentzcovitch et al.*, 2004], using the QHA [*Wallace*, 1972] and static elastic constants [*Núñez Valdez et al.*, 2010, 2011]. Computations are based on density functional theory within the local density approximation (LDA) [*Ceperley and Alder*, 1980]. Details about structure relaxation [*Wentzcovitch*, 1991] calculations can be found in previous publications [*Núñez Valdez et al.*, 2010, 2011]. VDoS were calculated using density functional perturbation theory [*Baroni et al.*, 2001], with the quantum-ESPRESSO [*Giannozzi et al.*, 2009]. At 10 different P's, dynamical matrices were obtained on a $2 \times 2 \times 2$ **q**-point mesh for one atomic configuration only. Force constants were interpolated on a $12 \times 12 \times 12$ regular **q**-point mesh to produce VDoS. This sampling is sufficient for accurate aggregate elastic properties [*Núñez Valdez et al.*, 2010; *Wu and Wentzcovitch*, 2011]. Free energies were computed exactly on a T-grid of 10 K spacing and interpolated on a P-grid of 0.1 GPa using third order finite strain expansions at every T. All P- and T-derivatives were computed on this grid. The main difference between this study and previous thermal elastic calculations using QHA free energies [*Karki et al.*, 1999; *Wentzcovitch et al.*, 2004] is that here C^T_{ijkl} are expressed analytically in terms of strain and mode Grüneisen parameters. Under the assumption that the angular distribution of strain Grüneisen parameters is isotropic, C^T_{ijkl} can be calculated without performing phonon calculations for strained configurations [*Wu and Wentzcovitch*, 2011]. This approximation is equivalent to assuming that thermal pressure is isotropic. Such assumption, although not exact, is implicit in the QHA [*Carrier et al.*, 2007, *Wentzcovitch et al.*, 2010] and can be quite accurate especially to address geophysical issues [*Carrier et al.*, 2008; *Wu and Wentzcovitch*, 2011], such as the high-PT dependence of $\frac{dlnV_S}{dT}$, which cannot be readily derived from experiments.

3. Results and Discussion

3.1. Aggregate Elastic Moduli of α- and β-$(Mg_{1-x},Fe_x)_2SiO_4$

[4] Our calculated averaged elastic moduli, K and G, shown as solid lines in Figure 1 (QHA valid region), agree very well with experimental data for both iron-free (Figures 1a and 1e) and iron-bearing ($x = 0.125$, Figures 1b and 1f) α- and β-phases [*Zha et al.*, 1996; *Isaak et al.*, 1989; *Li et al.*, 1996; *Zha et al.*, 1997; *Isaak et al.*, 2007; *Abramson et al.*, 1997; *Zha et al.*, 1998; *Isaak*, 1992; *Sinogeikin et al.*, 1998; *Li and Liebermann*, 2000; *Liu et al.*, 2009]. For $x = 0$, we find $K'_\alpha \approx 4.3$ and $G'_\beta \approx 1.6$ at ambient conditions [*On-line*, 2012], which are consistent with experimental values, 4.4 and 1.3, respectively [*Li et al.*, 1996]. Similarly calculated, $K'_\beta \approx 4.5$ and $G'_\beta \approx 1.6$ agree well with measurements of 4.2 and 1.5, respectively, by *Li et al.* [1996]. At ambient conditions, $K'_{\alpha,x=0.125} \approx 4.7$, $K'_{\beta,x=0.125} \approx 4.5$, and $G'_{(\alpha,\beta),x=0.125} \approx 1.5$. Besides, $K'_{x=0.125} \gg G'_{x=0.125}$ for both phases in the entire pressure interval considered [*On-line*, 2012]. These results suggest only minor effects of iron on the pressure derivatives of these elastic moduli.

[5] Figure 2 shows the temperature dependence of aggregate properties of α- and β-phases at 0 GPa. Within the valid

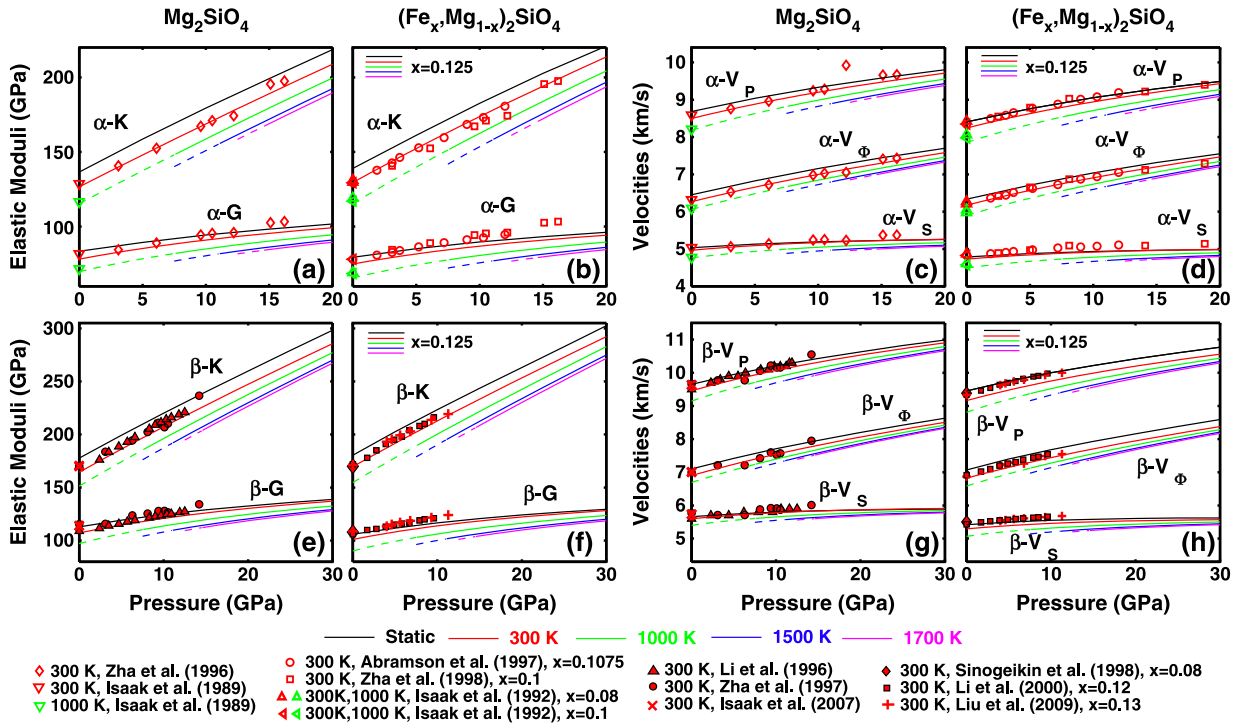

Figure 1. Pressure and temperature dependence of elastic moduli K and G (calculated as Voigt-Reuss-Hill averages [*Watt*, 1979]) and velocities V_P, V_S, and V_Φ for (a, c, e, g) Fe-free olivine-wadsleyite and (b, d, f, h) Fe-bearing olivine-wadsleyite. First-principles calculations within LDA (lines) are compared to available experimental data (symbols). Low-pressure-high temperature trends (dash lines) are outside the validity of the QHA.

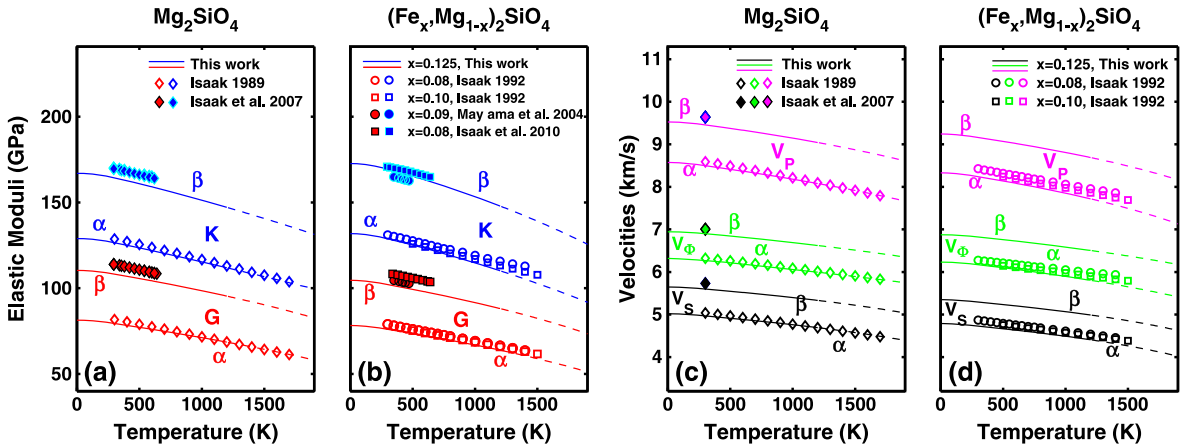

Figure 2. Temperature dependence of K, G, V_P, V_S, and V_Φ for (a, c) Mg end-members olivine-wadsleyite and (b, d) Fe-bearing olivine-wadsleyite. First-principles calculations within LDA (lines) are compared to available experimental data (symbols) at $P = 0$ GPa.

QHA regime (solid lines), the predictive power of our calculations is outstanding for the iron-free and iron-bearing α-phases (Figures 2a, 2b, 2c, and 2d), even though iron concentrations in experiments differ somewhat from $x = 0.125$ [*Isaak et al.*, 1989; *Isaak*, 1992]. For α- and β-phases, $\frac{d(K,G)}{dT} < 0$ with $\left|\frac{dK}{dT}\right| > \left|\frac{dG}{dT}\right|$ in the entire 300–1200 K temperature interval, irrespective of x [*On-line*, 2012].

[6] We also find that iron addition increases the bulk modulus, $[K_\alpha \approx (126.54 + 24x)$ GPa and $K_\beta \approx (164.37 + 42.2x)$ GPa], and decreases the shear modulus, $[G_\alpha \approx (78.17 - 26.2x)$ GPa and $G_\beta \approx (107.11 - 47.6x)$ GPa] for $0 \le x \le 0.125$ at ambient conditions [*On-line*, 2012]. These trends agree with experimental data for K_α and $G_{\alpha,\beta}$ (Figures 1a, 1b, 1e, and 1f, and 2a and 2b). But for K_β, the experimental determination is still unclear. Some studies suggest that K_β does not increase significantly with x [*Li et al.*, 1996; *Zha et al.*, 1997; *Isaak et al.*, 2007; *Sinogeikin et al.*, 1998; *Li and Liebermann*, 2000; *Liu et al.*, 2009] or maybe could even decrease [*Mayama et al.*, 2004; *Isaak et al.*, 2010] (Figure 2b). In contrast, calculations show clearly the dependence of K_β on x without ambiguity.

3.2. Effects of Iron and Temperature on Acoustic Velocities

[7] In the geophysics literature, the topography and seismic velocity anomalies at 410 km depth have been attributed mainly to lateral temperature variations [*Gu et al.*, 1998; *Houser and Williams*, 2010]. More recently, it has been recognized that the presence of water in variable amounts in the TZ [*Jacobsen*, 2006] can also affect topography and velocities in this region. Therefore, the interpretation of the origin of lateral variations in TZ [*Meier et al.*, 2009] depends crucially on the extent of the information available on various effects on velocities and on their accuracy. According to *Karato* [2011], the influence of water on seismic wave velocities is small compared with the effect of temperature, composition, and mineralogy changes at real mantle conditions [see e.g., *Irifune et al.*, 2008; *Weidner and Wang*, 2000]. The discussion on the effects of water velocity variations in TZ is still ongoing and will not be addressed in this paper. Here we only compare the effects of variations in iron concentration, x, and temperature on velocities at 13.5 GPa and 1700 K.

[8] Figures 1 and 2 show how acoustic velocities $[V_P = \sqrt{(K + \frac{4}{3}G)/\rho}$, $V_S = \sqrt{G/\rho}$, and $V_\Phi = \sqrt{(K/\rho)}]$ of α- and β-phases are affected by the ratio Fe/(Fe + Mg) = 0.125. At ambient conditions, V_P decreases by ~3% and V_S by ~5%. On the other hand, at 300 K and 0 GPa, a perturbation of 100 K results in a ~0.5–0.6% reduction in velocities (quite consistent with the ~0.7% reduction reported by *Karato* [2011]). At ~410 km depth, this perturbation is reduced to ~0.3–0.4% only. This can also be seen from the variation of $\frac{dlnV_S}{dT}$ with pressure. For instance, $\frac{dlnV_{S,\alpha}}{dT}\Big|_{x=0(x=0.125)} = -5 \times 10^{-5}\,K^{-1}(-6 \times 10^{-5}\,K^{-1})$ at ambient conditions but $-4 \times 10^{-5}\,K^{-1}(-5 \times 10^{-5}\,K^{-1})$ at ~410 km depth conditions. Similar values can be found for wadsleyite [*On-line*, 2012]. Thus, the effect of lateral temperature variations on velocities decreases with pressure, while the effect of variation in x increases. For example, at ~410 km depth, the effect of a ~100 K perturbation on velocities is comparable to an increase in x by ~1% only. Therefore, mineralogy, such as variations in iron concentration in different phase assemblages, should be an important source of lateral velocity heterogeneities in the UM and TZ.

3.3. Effect of Iron Heterogeneity on Discontinuities across the $\alpha \rightarrow \beta$ Transition

[9] Accurate data on elasticity of α- and β-$(Mg_{1-x},Fe_x)_2SiO_4$ at UM and TZ conditions are critical for investigating the role of the $\alpha \rightarrow \beta$ transformation on the 410 km seismic discontinuity. Predicted contrasts, Δ, for a property M with iron content x across the $\alpha \rightarrow \beta$ transformation, $\Delta M = 2(M_{x,\beta} - M_{x,\alpha})/(M_{x,\alpha} + M_{x,\beta}) \times 100$, show important differences in elastic moduli and velocities between these two phases near 410 km depth conditions (Table 1). The reconstructive $\alpha \rightarrow \beta$ transition, which involves the pairing of isolated SiO_4 units in α to form Si_2O_7 dimers in β, substantially strengthens K and G (Figures 1a, 1b, 1e, and 1f). For example, at 1700 K and 13.5 GPa, $\Delta K_{x=0} = 20.1\%$ and $\Delta G_{x=0} = 28.1\%$ (Table 1). In the presence of iron ($x = 0.125$), these contrasts decrease. As a result, velocity contrasts ΔV_P and ΔV_S decrease by 5.5% and 7.0%, respectively. Thus, the effect

Table 1. Predicted Contrasts in % Across the $\alpha \rightarrow \beta$ Transition at 13.5 GPa

T (K)	1500		1700	
x	0.0	0.125	0.0	0.125
$\Delta\rho$	5.4	5.2	5.4	5.3
ΔK	20.0	19.6	20.1	19.7
ΔG	28.0	26.3	28.1	26.4
ΔV_P	9.0	8.5	9.1	8.6
ΔV_S	11.4	10.6	11.4	10.6
ΔV_Φ	7.3	7.2	7.4	7.3
$\Delta(\rho V_P)$	14.4	14.2	14.5	14.3
$\Delta(\rho V_S)$	16.7	16.6	16.8	16.7

of a change of 12.5% in iron concentration on contrasts is much larger than the effect of a 200 K in temperature variation at fixed composition (Table 1). We can also see that, at ambient conditions(*) and 1700 K and 13.5 GPa(†), lateral temperature variations cause heterogeneity ratios $\left(R_{A/B} = \frac{\delta \ln V_A}{\delta \ln V_B}\right)$ of $R^{\alpha}_{S/P,x=0(x=0.125)} \sim [1.28(1.05)]^*$ versus $[1.20(1.39)]^\dagger$, $R^{\alpha}_{\Phi/S,x=0(x=0.125)} \sim [0.79(0.77)]^*$ versus $[0.72(0.69)]^\dagger$, $R^{\beta}_{S/P,x=0(x=0.125)} \sim [1.27(1.04)]^*$ versus $[1.18(1.81)]^\dagger$, and $R^{\beta}_{\Phi/S,x=0(x=0.125)} \sim [0.81(0.78)]^*$ versus $[0.75(0.48)]^\dagger$. For comparison, at 0 K between 0 and 13.5 GPa, $R^{\alpha}_{S/P} \sim 1.54 - 1.67$, $R^{\alpha}_{\Phi/S} \sim 0.37 - 0.34$, $R^{\beta}_{S/P} \sim 1.99 - 2.16$, and $R^{\beta}_{\Phi/S} \sim 0.1 - 0.09$ due to iron heterogeneity [*Núñez Valdez et al*., 2010, 2011]. All these results show that iron heterogeneity is more effective than lateral temperature variations in producing observed velocity heterogeneity ratios in α- and β- phases separately and across the $\alpha \rightarrow \beta$ transition. Obviously, these results should be affected by the presence of coexisting phases. If the interaction between the olivine system and coexisting phases (i.e., garnet, pyroxenes, and $CaSiO_3$) is negligible, this conclusion should still hold, although these ratios could change somewhat.

[10] We also find that velocity contrasts across the transition are essentially unaffected by pressure, i.e., alone the topography of the "410 discontinuity" should not affect velocity contrasts. This is consistent with inferences from experiments at 300 K in iron-free samples [*Li et al*., 1996; *Zha et al*., 1997]. Also, $\Delta\rho$ and ΔK are not significantly affected by iron (Table 1). Therefore, the mantle aggregate at 410 km depth will have $\Delta\rho$ reduced (buffered) from the current value of ~5.3% (at 1700 K and 13.5 GPa) for pure olivine to ~3% in an aggregate with 60 vol % of olivine, as in pyrolite (a simple derivation can be found in [*Yu et al*., 2008]). This is consistent with the 0.2–4% density increase at 410 km depth from the seismic study by *Shearer and Flanagan* [1999]. Compared to the Mg end-members, overall the presence of iron decreases only slightly contrasts in properties across the transition. We also conclude that velocities contribute more than density to *P*- and *S*-impedance contrasts (see Table 1).

4. Conclusions

[11] We presented extensive first-principles results for aggregate elastic properties and sound velocities of α- and β-$(Fe_x,Mg_{1-x})_2SiO_4$, with variable x at relevant mantle conditions. A novel semi-analytical method used here [*Wu and Wentzcovitch*, 2011] expedited the thermal elasticity calculation by approximately 2 orders of magnitude compared to QHA-based calculations [e.g., *Wentzcovitch et al*., 2004]. We showed the difference between physical properties at ambient conditions and conditions expected near the 410 km seismic discontinuity. In overall, we showed the importance of using accurate thermal elasticity data obtained at local conditions and compositions prevailing in the mantle in the interpretation of seismic data. We concluded that variation in iron concentration might impact more significantly than temperature variation on velocity heterogeneity ratios, including discontinuity ratios at ~410 km depth. Other chemical and phase heterogeneities, such as variations in amounts of aluminum and calcium-bearing minerals, should presumably have similar effects. Finally, calculated contrasts in properties across the 410 km discontinuity indicate that compressional and shear impedance contrasts are caused primarily by velocity discontinuities rather than density discontinuity.

[12] **Acknowledgments.** Research is supported by the NSF/EAR-1019853 and EAR-0810272. Computations were performed using the ***VLab*** cyberinfrastructure at the Minnesota Supercomputing Institute.

References

Abramson, E. H., J. M. Brown, L. J. Slutsky, and J. Zaug (1997), The elastic constants of San Carlos olivine to 17 GPa, *J. Geophys. Res.*, *102*, 12253–12263.

Akaogi, M., E. Ito, and A. Navrotsky (1989), Olivine-modified spinel-spinel transitions in the system Mg_2SiO_4-Fe_2SiO_4: Calorimetric measurements, thermochemical calculation, and geophysical application, *J. Geophys. Res.*, *94*, 15 671–15 685.

Baroni, S., A. Dal Corso, S. de Gironcoli, and P. Gianozzi (2001), Phonons and related crystal properties from density-functional perturbation theory, *Rev. Mod. Phys.*, *73*(2), 515 LP–562 LP.

Brown, J. M., and T. J. Shankland (1981), Thermodynamic parameters in the Earth as determined from seismic profiles, *Geophys. J. R. Astron. Soc.*, *66*, 579–596.

Carrier, P., J. F. Justo, and R. M. Wentzcovitch (2008), Quasiharmonic elastic constants corrected for deviatoric thermal stresses, *Phys. Rev. B*, *78*, 144302-1–144302-6.

Carrier, P., R. M. Wentzcovitch, and J. Tsuchiya (2007), First principles prediction of crystal structures at high temperatures using the quasiharmonic approximation, *Phys. Rev. B 76*, 064116.

Ceperley, D. M., and B. J. Alder (1980), Ground state of the electron gas by a stochastic method, *Phys. Rev. Lett.*, *45*, 566–569.

Da Silva, C. R. S., P. R. C. da Silveira, B. B. Karki, R. M Wentzcovitch, P. A. Jensen, E. F. Bollig, M. Pierce, G. Erlebacher, and D. A. Yuen (2007), Virtual laboratory for planetary materials: System service architecture overview. *Phys. Earth Planet. Inter.*- Special Issue: Computational Challenges, *163*, 321–332.

Da Silveira, P., M. Núñez Valdez, R. M. Wentzcovitch, M. Pierce, and D. A. Yuen (2011), Virtual laboratory for planetary materials (VLab): An updated overview of system service architecture, in TG'11 Proceedings of the 2011 TeraGrid Conference: Extreme Digital Discovery, ACM, New York, NY, USA.

Da Silveira, P., C. R. S. da Silva, and R. M. Wentzcovitch (2008), Metadata management for distributed first principles calculations in VLab—A collaborative cyberinfrastructure for materials computation, *Comp. Phys. Commun.*, *178*, 186–198.

Giannozzi P., et al. (2009), QUANTUM ESPRESSO: A modular and open-source software project for quantum simulations of materials, *J. Phys. Condens. Matter*, *21*, 395502. http://www.quantum-espresso.org

Gu, Y., A. M. Dziewonski, and C. B. Agee (1998), Global de-correlation of the topography of transition zone discontinuities, *Earth Planet. Sci. Lett.*, *157*, 57–67.

Houser, C., and Q. Williams (2010), Reconciling Pacific 410 and 660 km discontinuity topography, transition zone shear velocity patterns, and mantle phase transitions, *Earth. Planet. Sci. Lett.*, *296*(3), 255–266.

Irifune, T., Y. Higo, T. Inoue, Y. Kono, H. Ohfuji, and K. Funakoshi (2008), Sound velocities of majorite garnet and the composition of the mantle transition region, *Nature*, *451*, 814–817.

Irifune, T., and A. E. Ringwood (1987), Phase transformations in primitive MORB and pyrolite compositions to 25 GPa and some geophysical implications, in *High Pressure Research in Geophysics*, edited by

M. Manghnani and Y. Syono, pp. 231–242, TERRAPUB/AGU, Tokyo/Washington, D.C.

Isaak, D. G. (1992), High-temperature elasticity of iron-bearing olivines, *J. Geophys. Res.*, *97*, 1871–1885.

Isaak, D. G., O. L. Anderson, T. Goto, and I. Suzuki (1989), Elasticity of single-crystal forsterite measured to 1700 K, *J. Geophys. Res.*, *94*, 5895–5906.

Isaak, D. G., G. D. Gwanmesia, M. G. Davis, S. C. Stafford, A. M. Stafford, and R. S. Triplett (2010), The temperature dependence of the elasticity of Fe-bearing wadsleyite, *Phys. Earth Planet. Inter.*, *182*, 107–112.

Isaak, D. G., G. D. Gwanmesia, D. Falde, M. G. Davis, R. S. Triplett, and L. Wang (2007), The elastic properties of β-Mg_2SiO_4 from 295 to 660 K and implications on the composition of Earth's upper mantle, *Phys. Earth Planet. Inter.*, *162*, 22–37.

Jacobsen, S. D. (2006), Effect of water on the equation of state of nominally anhydrous minerals, in *Water in Nominally Anhydrous Minerals*, Rev. in Mineral. and Geoch., vol. *62*, pp. 321–342, edited by H. Keppler and J. R. Smyth, Mineralogical Society of America.

Karato, S. (2011), Water distribution across the mantle transition zone and its implications for global material circulation, *Earth Planet. Sci. Lett.*, *301*(3), 413–423.

Karki, B. B., R. M. Wentzcovitch, S. de Gironcoli, and S. Baroni (1999), First principles determination elastic anisotropy and wave velocities of MgO at lower mantle conditions, *Science*, *286*, 1705.

Katsura, T., and E. Ito (1989), The system Mg_2SiO_4-Fe_2SiO_4 at high pressures and temperatures: Precise determination of stabilities of olivine, modified spinel and spinel. *J. Geophys. Res.*, *94*, 15 663–15 670.

Li, B., G. D. Gwanmesia, and R. C. Liebermann (1996), Sound velocities of olivine and beta polymorphs of Mg_2SiO_4 at Earth's transition zone pressures, *Geophys. Res. Lett.*, *23*, 2259–2262.

Li, B., and R. C. Liebermann (2000), Sound velocities of wadsleyite β-$(Mg_{0.88},Fe_{0.12})_2SiO_4$ to 10 GPa, *Am. Mineral.*, *85*, 292–295.

Li, B., and R. C. Liebermann (2007), Indoor seismology by probing the Earth's interior by using sound velocity measurements at high pressures and temperatures, *Proc. Natl. Acad. Sci.*, *104*, 9145–9150.

Li, L., D. J. Weidner, J. Brodholt, D. Alfè, G. D. Price, R. Caracas, and R. Wentzcovitch (2006), Phase stability of $CaSiO_3$ perovskite at high pressure and temperature: Insights from ab initio molecular dynamics, *Phys. Earth Planet. Inter.*, *155*, 260–268.

Liu, W., J. Kung, and B. Li (2005), Elasticity of San Carlos olivine to 8GPa and 1073 K, *Geophys. Res. Lett.*, *32*, L16301.

Liu, W., J. Kung, B. Li, N. Nishiyma, and Y. Wang (2009), Elasticity of β-$(Mg_{0.87},Fe_{0.13})_2SiO_4$ wadsleyite to 12 GPa and 1073 K, *Phys. Earth Planet. Inter.*, *174*, 98–104.

Mayama, N., I. Suzuki, and T. Saito (2004), Temperature dependence of elastic moduli of β-$(Mg_{1-x},Fe_x)_2SiO_4$, *J. Geophys. Res.*, *31*, L04612.

Meier, U., J. Trampert, and A. Curtis (2009), Global variations of temperature and water content in the mantle transition zone from higher mode surface waves, *Earth. Planet. Sci. Lett.*, *282*, 91–101.

Núñez Valdez, M., P. da Silveira, and R. M. Wentzcovitch (2011), Influence of iron on the elastic properties of wadsleyite and ringwoodite, *J. Geophys. Res.*, *116*, B12207.

Núñez Valdez, M., K. Umemoto, and R. M. Wentzcovitch (2010), Fundamentals of elasticity of $(Mg_{1-x},Fe_x)_2SiO_4$-olivine, *Geophys. Res. Lett.*, *37*, L14308.

Oganov A. R., J. P. Brodholt, and J. P. Price (2001), The elastic constants of MgSiO3 perovskite at pressures and temperatures of the Earth's mantle, *Nature*, *411*, 934–937.

On-line data from this work (2012), [Available at http://www.vlab.msi.umn.edu/resources/thermoelasticity/index.shtml].

Putnis, A. (1992), *Introduction to Mineral Sciences*, 399 pp., Cambridge University Press, UK.

Ringwood, A. E. (1975), *Composition and Petrology of the Earth's Mantle*, 618 pp., McGraw-Hill, New York.

Shearer, P. M., and M. P. Flanagan (1999), Seismic velocity and density jumps across the 410- and 660-kilometer discontinuities, *Science 285*(5433), 1545–1548.

Sinogeikin, S. V., T. Katsura, and J. D. Bass (1998), Sound velocities and elastic properties of Fe-bearing wadsleyite and ringwoodite, *J. Geophys. Res.*, *103(*B9*)*, 20,819–20,825.

Stackhouse, S., L. Stixrude, and B. B. Karki (2010), Determination of the high-pressure properties of fayalite from first-principles calculations, *Earth Planet. Sci. Lett. 289*, 449–456.

Wallace, D. C. (1972), *Thermodynamics of Crystals*, 20 pp., John Wiley& Sons, Inc., USA.

Watt, J. P. (1979), Hashin-Shtrikman bounds on the effective elastic moduli of polycrystals with orthorhombic symmetry, *J. Appl. Phys.*, *50*, 6290–6295.

Weidner, D. J., and Y. Wang (2000), Phase transformations: Implications for mantle structure, in *Earth's Deep Interior: Mineral Physics and Tomography from the Atomic to the Global Scale*, Geophys. Monogr., vol. *117*, edited by S. Karato et al., pp. 215–235, AGU, Washington, D.C.

Wentzcovitch, R. M. (1991), Invariant molecular dynamics approach to structural phase transitions, *Phys. Rev. B*, *44*, 2358–2361.

Wentzcovitch, R. M., B. B. Karki, M. Cococcioni, and S. de Gironcoli (2004), Thermoelastic properties of $MgSiO_3$-perovskite: Insights on the nature of the Earth's lower mantle, *Phys. Rev. Lett.*, *92*, 018501.

Wentzcovitch, R. M., Z. Wu, and P Carrier (2010), First principles quasiharmonic thermoelasticity of mantle minerals, *Rev. Mineral. Geochem.*, *71*, 99–128.

Wu, Z., and R. M. Wentzcovitch (2011), Quasiharmonic thermal elasticity of crystals: An analytical approach. *Phys. Rev. B 83*, 184115.

Yu, Y. G., Z. Wu, and R. M. Wentzcovitch (2008), $\alpha \leftrightarrow \beta \leftrightarrow \gamma$ transformations in Mg_2SiO_4 in Earth's transition zone, *Earth Planet. Sci. Lett.*, *273*, 115–122.

Zha, C. S., T. S. Duffy, R. T. Downs, and H. K. Mao (1996), Sound velocity and elasticity of single-crystal forsterite to 16 GPa, *J. Geophys. Res.*, *101*, 17535–17545.

Zha, C. S., T. S. Duffy, R. T. Downs, H. K. Mao, and R. J. Hemley (1998), Brillouin scattering and X-ray diffraction of San Carlos olivine: Direct pressure determination to 32 GPa, *Earth Planet. Sci. Lett.*, *159*, 25–33.

Zha, C. S., T. S. Duffy, H. W. Mao, R. T. Downs, R. J. Hemley, and D. J. Weidner (1997), Single-crystal elasticity of β-Mg_2SiO_4 to the pressure of the 410 km seismic discontinuity in the earth's mantle, *Earth Planet. Sci. Lett.*, *147*, E9–E15.